Large-Amplitude Vibrations of Spider Web Structures

Kaewunruen, Sakdirat; Ngamkhanong, Chayut; Yang, Tianyu

DOI:
10.3390/app10176032

Document Version
Publisher's PDF, also known as Version of record

Citation for published version (Harvard):
Kaewunruen, S, Ngamkhanong, C & Yang, T 2020, 'Large-Amplitude Vibrations of Spider Web Structures', *Applied Sciences (Switzerland)*, vol. 10, no. 17, 6032. https://doi.org/10.3390/app10176032

applied sciences

MDPI

Article

Large-Amplitude Vibrations of Spider Web Structures

Sakdirat Kaewunruen [1,*], Chayut Ngamkhanong [1] and Tianyu Yang [2]

[1] Department of Civil Engineering, School of Engineering, University of Birmingham, Birmingham B15 2TT, UK; cxn649@bham.ac.uk
[2] Arch-Age Design, Jiulongpo District, Chongqing 400039, China; stacy2@live.cn
* Correspondence: s.kaewunruen@bham.ac.uk

Received: 14 August 2020; Accepted: 28 August 2020; Published: 31 August 2020

Featured Application: The new findings exhibit for the first time the nonlinear dynamic phenomena of spider web systems subject to large amplitude precursors stemming from extreme winds, large deformation, material imperfections, hostile climatic conditions and so on. This study enables new discoveries and insights by enhancing large deformable finite elements with energy method. The novel insights can be used (not limited to) as a reference for the analysis, design, inspection and maintenance of structural membranes, netting cables (or cable-like structures such as rail overhead conductors), tensegrity structures, soft tissues and soft matter, and other bio-inspired structures.

Abstract: Spider silk, as a natural material, shows exceptional performance in its properties. The combination of the superior properties of spider silk and the geometry of spider structures make the spider web very resilient. A spider web structure can be considered as a cable-like structure with inappreciable torsional, bending and shear rigidities. An investigation emphasising on natural frequencies and corresponding mode shapes with and without the consideration of geometric nonlinearity is presented in this paper. This study is the world's first discovery of large amplitude free vibration behaviours of spider web structures. Large deformable finite element 3D models of spider web structures have been developed and validated. By using the energy method, the variational model of the spider web structures have been established to further extend the finite element model, consisting of the strain energy due to axial deformation, kinetic energy due to the spider web movement and the virtual work caused by the self-weight per unit unstretched length. The emphasis of this study is placed on the linear and geometric nonlinear behaviour of the spider web structures considering different structural patterns and material properties. To determine the large-amplitude free vibrational behaviours, a series of pretension load is applied to the first step in Abaqus to initiate the nonlinear strain-displacement relationships enabling a precursor to free vibrations. The parametric studies stemming from structural patterns (the number of radial and capture threads), elastic modulus, density, and inertia moment have been highlighted. The insight will help engineers and scientists to adapt the concept of spider webs, their geometric properties, and damage patterns for the design of any structural membranes, preventing any failure from dynamic resonances and nonlinear phenomena.

Keywords: nonlinear free vibration; natural frequencies; mode shapes; nonlinear geometric behaviour; nonlinear dynamics; spider web

1. Introduction

The function of a spider web is to capture and hold a rapidly flying insect, which shows that the spider web has excellent flexibility and resilience. Two aspects of the design of the web make this possible: the optimised spider silk and the design of the web. Spider silk is one of

the bio-inspired materials that have shown excellent performance exceeding artificial materials in their properties [1]. There has been interest in adopting the spider web's engineering properties in defence technology and medical applications, including microscopes, telescopes and bomb guiding systems [2]. Considering it on a weight to weight basis, its tensile strength is sometimes even stronger than steel and some silks are almost as elastic as rubber. On this ground, silks provide two to three times toughness of synthetic fibres such as nylon or Kevlar. Unlike man-made polymers, spider silk can improve in strength without compromising fracture toughness [3]. Besides the superior material properties of spider silk, spider web structures themselves can be recognised as a pre-stressed system called tensegrity (tensional integrity) structures [4]. This sort of structure shows a unique combination of geometry and mechanic properties, and as a result of the optimal distribution of structural mass, they are highly efficient structures. It is the nature of spider web structures to quickly absorb the energy as well as constrain drastic oscillations due to the prey impact [5]. The experiments on energy absorption and dissipation of spider web subjected to flying prey have been studied considering different species of spiders [6–8]. Moreover, localised damage is a universal feature of spider webs. When a spider web is subjected to local loading, failure is limited to the loading threads and the loaded thread becomes a sacrificial element to keep the majority of the web remains intact, and spider webs strength after slightly damaged [9]. The spider web is so resilient because of its distinctive combination of strength and stretchiness and the geometrical arrangement of the web. It is noted that the properties of spider silk have been fully studied [10–12]. However, many researchers only focused on the outstanding properties of silk rather than the spider web's structure itself.

It is noticeable that the spider web could experience large deformation due to wind load or prey trapping [13]. It should be noted that the spider web should be able to trap large prey. This effect allows the web to absorb high kinetic impacts that would otherwise cause an extension above the elastic range and therefore destroy the web. The single degree of freedom experiment has been performed to evaluate the stiffness and damping decay of spider web and it is found that the overall stiffness of the spider web tends to be nonlinear under shock load [14]. Nevertheless, the studies of the structural behaviour using advanced finite element modelling regarding the vibration characteristics of spider webs have not been fully investigated. Hence, this study investigates the large amplitude free vibration behaviour of the spider web structure. This better insight into its engineering performance can unleash its applications in battle and defence technology. The large-deformable finite element 3D models of spider web structures with and without geometric nonlinearities are developed using Abaqus. According to the virtual work-energy theory, the model is formed from the strain energy owe to axial deformation, kinetic energy owes to the spider web movement and the virtual work due to the self-weight per unit unstretched length, and the concept of large-strain, the large-deformation principle has been used to evaluate natural frequencies and corresponding mode shapes with geometric nonlinearity. To analyse the performance of spider webs, several parametric studies of the effect of different patterns, elastic modulus, density, and inertia moment were carried out.

2. Materials and Methods

2.1. Equations of Motion

The concept of cable structure can be applied to spider silk since the structure of spider silk is naturally a special class of prestressed system called tensional integrity (tensegrity). Hence, to investigate the vibration responses of spider silk, the strain energy method considering only axial deformation was applied. The states of spider silk can be divided into three states: unstretched state, equilibrium state, and dynamic or displaced state. The first state is the initial unstretched state dS at (x,y). After tension applied, the cable is elongated and the structure moves to the equilibrium state at dS0 at (x_0,y_0). On account of free vibration at dynamic or displaced state $d\bar{s}$, spider silk displaces to the position of ($x_0 + u$, $y_0 + v$, w), in which u, v and w are the hypothetic displacements in the direction of x, y and z-axis,

respectively [15]. The length of ds_0 is an infinitesimal spider silk element, and the equilibrium state can be represented as

$$ds_0{}^2 = dx_0{}^2 + dy_0{}^2 \text{ or } ds_0 = \sqrt{1+\dot{y}_0^2}dx_0, \tag{1}$$

Similarly, the equation of displaced state $d\bar{s}$ can be written as

$$d\bar{s} = \sqrt{\left(1+\dot{u}\right)^2 + \left(\dot{y}_0+\dot{v}\right)^2 + \dot{w}^2}dx_0, \tag{2}$$

where $\dot{u} = \frac{du}{dx}$, $\dot{v} = \frac{dv}{dx}$, $\dot{w} = \frac{dw}{dx}$.

Total strain due to stretching of the cable can be derived at the displaced state by

$$\bar{\varepsilon} = \frac{d\bar{s}-ds}{ds} = \frac{(1+\varepsilon_0)}{\sqrt{1+\dot{y}_0^2}}\sqrt{\left(1+\dot{u}\right)^2 + \left(\dot{y}_0+\dot{v}\right)^2 + \dot{w}^2} - 1, \tag{3}$$

where ε_0 is the initial static strain.

The strain energy equation taking dissipated energy due to stretching of the cable can be written as

$$\begin{aligned}\delta U = \int_0^{X_H}\Big(&\Big(\frac{EA(1+\varepsilon_0)\dot{u}+EA}{\sqrt{1+\dot{y}_0^2}} - \frac{EA(1+\dot{u})}{\sqrt{(1+\dot{u})^2+(\dot{y}_0+\dot{v})^2+\dot{w}^2}}\Big)\delta u' \\ &+\Big(\frac{EA(1+\varepsilon_0)\dot{v}+EA\dot{y}_0}{\sqrt{1+\dot{y}_0^2}} - \frac{EA(\dot{y}_0+\dot{v})}{\sqrt{(1+\dot{u})^2+(\dot{y}_0+\dot{v})^2+\dot{w}^2}}\Big)\delta v' + \Big(\frac{EA(1+\varepsilon_0)(\dot{w})}{\sqrt{1+\dot{y}_0^2}} - \frac{EA\dot{w}}{\sqrt{(1+\dot{u})^2+(\dot{y}_0+\dot{v})^2+\dot{w}^2}}\Big)\delta w'\Big)dx_0,\end{aligned} \tag{4}$$

The virtual work done by inertial force can be derived by

$$\delta W_i = -\int_0^l \frac{m\sqrt{1+\dot{y}_0^2}}{g(1+\varepsilon_0)}\left(\ddot{u}\delta u + \ddot{v}\delta v + \ddot{w}\delta w\right)dx_0, \tag{5}$$

Total energy ($\delta\Pi$) can be derived by [15]

$$\delta\Pi = \delta U - \delta W_i = 0, \tag{6}$$

where $\delta\Pi$ is the total energy, δU is a variation of strain energy, δW_i is the virtual work done due to initial force.

The pinned support conditions are applied at both ends of the silk member so that the boundary conditions are $\delta u = \delta v = \delta w = 0$ when $x_0 = 0$ and $x_0 = l$. After substituting the boundary conditions and equilibrium conditions ($\delta\dot{u} = \delta\dot{v} = \delta\dot{w} = \delta\ddot{u} = \delta\ddot{v} = \delta\ddot{w} = 0$) into the total energy equation, the governing equations of motions can be expressed as shown in Equations (7)–(9). These equations are used to analyse the three-dimensional large amplitude free vibration with the undamped system.

$$\left[\frac{EA(1+\varepsilon_0)\dot{u}+EA}{\sqrt{1+\dot{y}_0^2}} - \frac{EA\left(1+\dot{u}\right)}{\sqrt{\left(1+\dot{u}\right)^2+\left(\dot{y}_0+\dot{v}\right)^2+\dot{w}^2}}\right]' - \frac{m\sqrt{1+\dot{y}_0^2}}{g(1+\varepsilon_0)}\ddot{u} = 0, \tag{7}$$

$$\left[\frac{EA(1+\varepsilon_0)\dot{v}+EA\dot{y}_0}{\sqrt{1+\dot{y}_0^2}} - \frac{EA\left(\dot{y}_0+\dot{v}\right)}{\sqrt{\left(1+\dot{u}\right)^2+\left(\dot{y}_0+\dot{v}\right)^2+\dot{w}^2}}\right]' - \frac{m\sqrt{1+\dot{y}_0^2}}{g(1+\varepsilon_0)}\ddot{v} = 0, \tag{8}$$

$$\left[\frac{EA(1+\varepsilon_0)\left(\dot{w}\right)}{\sqrt{1+\dot{y}_0^2}} - \frac{EA\dot{w}}{\sqrt{\left(1+\dot{u}\right)^2+\left(\dot{y}_0+\dot{v}\right)^2+\dot{w}^2}}\right]' - \frac{m\sqrt{1+\dot{y}_0^2}}{g(1+\varepsilon_0)}\ddot{w} = 0, \tag{9}$$

2.2. Modelling of Spider Web

Many researchers have investigated the mechanical properties of spider silk. In this model, radial and spiral captured threads are made of dragline silk of the *Argiope aurantia* spider with a circular fibre diameter of 4 microns. Generally, spiral threads are made of viscid silk which has lower strength but higher extensibility than dragline silk and this combination optimise the function of a spider web. However, in this research, we focussed on the structure behaviour itself, therefore, the same material properties were applied on both radial and spiral thread. The material properties of spider web used are listed in Table 1 [4].

Table 1. Engineering properties of the *A. aurentia* silk [4].

Material	Density (kg/m^3)	Tensile Modulus (GPa)	Poisson's Ratio	Strength (GPa)	Strain (%)
A. aurantia silk	1098	34	0.49	1.75	26

A large-deformable finite element model of spider web structures with geometric nonlinearities was developed using Abaqus based on the typical spider web structure. It is noted that there are two main thread elements in the spider web structure: spiral thread and radial thread as shown in Figure 1 [9]. The structural performance is dominated by the radial thread while the spiral tread acts as a non-structural member so that higher forces are required to break the radial thread. Based on the finite element method, both relatively simple linear problems and nonlinear analysis can be solved. The spider web model was developed on a 2-D plane (X and Y axis), but it is a 3-D model because the free vibration of the spider web would happen on the third axis, Z. The analysis is divided into two parts: linear analysis and nonlinear analysis. For linear analysis, five different patterns of spider web were built to compare the effects of different parameters and structural patterns on natural frequencies and corresponding mode shapes. For nonlinear analysis, natural frequencies extracted from large amplitude free vibration and corresponding mode shapes were investigated, taking geometric nonlinearities into account.

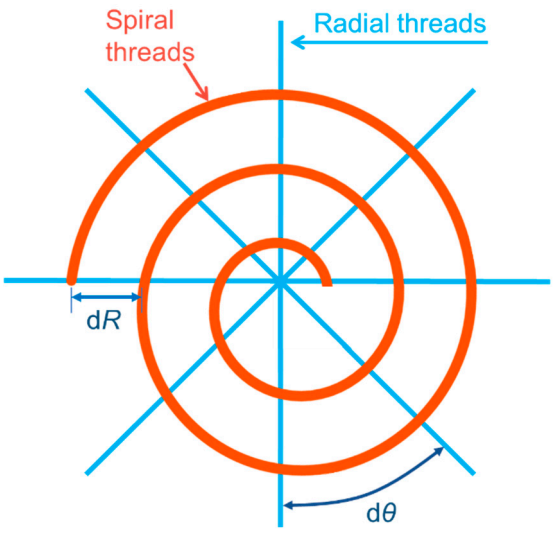

Figure 1. Typical spider web geometry.

In this study, six patterns of spider web structure were studied, as presented in Figure 2. The spider web structure is constructed based on the actual dimensions in previous study [14]. The radii of spiral threads are 0.3 m and the length of each radial thread is 0.4 m. The overall size of the model is 0.8 m × 0.8 m. The spacing between adjacent spiral threads is 0.03 m for all patterns except patterns 5 and 6 which have the spacing of 0.015 and 0.01 m, respectively. The ratio of the spiral to radial thread diameter is 1 and the angle between the radial thread is 45, 30 and 22.5 degrees in patterns 1, 2 and 3,

respectively. Patterns 4 and 5 have the same angle as pattern 1 and its capture threads are series of concentric circles instead of spiral threads.

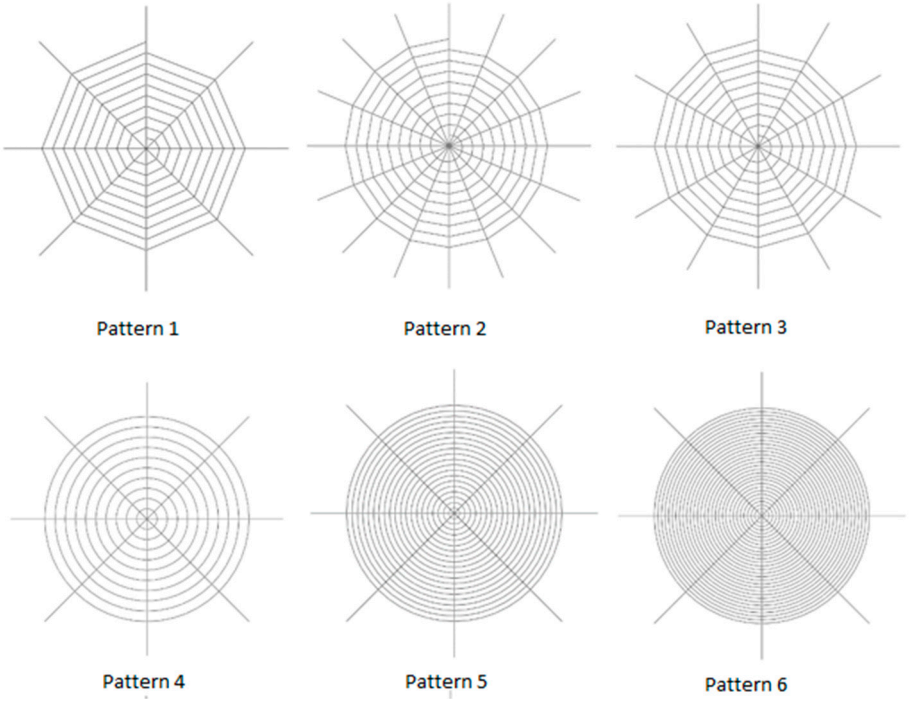

Figure 2. Patterns of spider web.

At first, the spider web was modelled as a truss structure, which means the member only carries tensile and compressive axial loads without rotation and torque. In addition, truss elements only need to set the cross-sectional area to define element properties in ABAQUS. As mentioned before, the spider web was modelled on a 2-D plane while vibrating in a third axis (Z axis), but ABAQUS could not analyse the frequencies without mass and stiffness matrix on the third axis. Hence, beam elements were applied instead. Beam element is usually defined by stiffness (K), torque (J), and moment of inertia (I), but for spider silk, a sort of cable-type element, the bending, torsional and shear rigidities should be as small as possible. The boundary conditions exhibited the characteristic of spider web anchorages. From a structural engineering view mentioned in [16], a spider web is a cable structure whose segments only sustain tension. Therefore, the boundary condition of spider web structure is similar to the cable structure, which is a pinned support that only permits rotation. It should be pointed out that the boundary condition was applied to the initial step. Moreover, mesh convergence analysis was first performed by resizing the element size from 0.01 to 0.2 m to generate a proper mesh size and accurately compute the FEM results. It is noted that the automated meshing can clearly provide the proper mesh size, as presented in Figure 3. It is noted that the proper mesh size is 23 mm, which was generated automatically in ABAQUS.

The linear model extracts natural frequencies due to free vibration. It should be noted that linear analysis can properly analyse the structural responses restricted to small deformation so that the small deformation and constant stiffness are the fundamental assumptions of linear analysis. However, the stiffness may change when the structure is subjected to large deformation. In this model, geometric nonlinearity is considered. The so-called geometric nonlinearity is that the varying geometric configuration can cause nonlinear behaviour when a structure experiences large deformations [17]. It includes the effect of large displacement and rotations, snap through, and load stiffening. Therefore, along with the Nlgeom setting, pretension loads which can change the structural stiffness need to be applied to the structure to set a geometric nonlinearity as the initial condition of the second step.

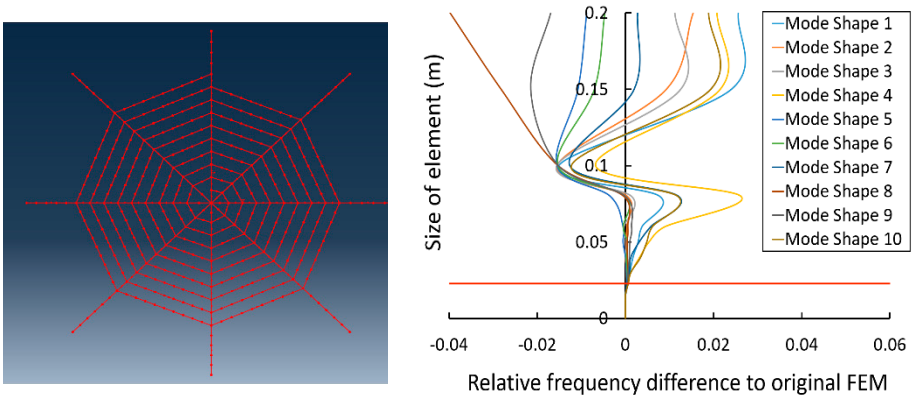

Figure 3. (**a**) Mesh generation (**b**) mesh convergence analysis.

2.3. Model Validation

Due to the characteristic of actual spider webs that are very complex and have different shapes depending on their types, the accuracy of measurement requires a high level of model accuracy. Hence, the spider web model is first compared with the previous models [18]. Several models of artificial spider webs were previously developed in ANSYS to understand the relationship between natural frequency and the mechanical properties of a spider web. It is noted that nylon and rubber properties were used for the radial and spiral threads in the artificial spider web, respectively. The model consisted of 16 nylon radial threads and 12 rubber spiral threads with the spacing of 15 mm. The spacing between the rubber spiral threads was 15 mm. The diameter of spider silk and its elastic modulus was adopted to 500–800 μm and 3 GPa, respectively, to match the relevant data [18]. Therefore, a comparison based on their data could be used to validate the current model. The model was built with an identical pattern to the previous models used in [18] (Figure 4). The comparison results are presented in Figure 5.

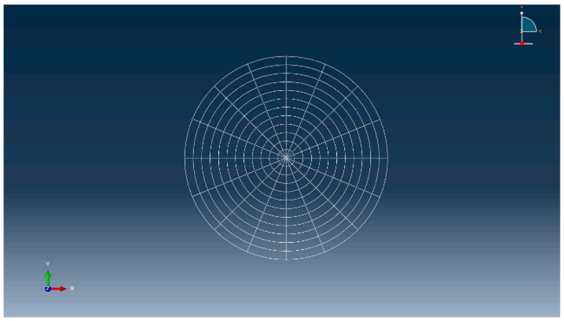

Figure 4. Structure of a nylon-rubber artificial web for model validation.

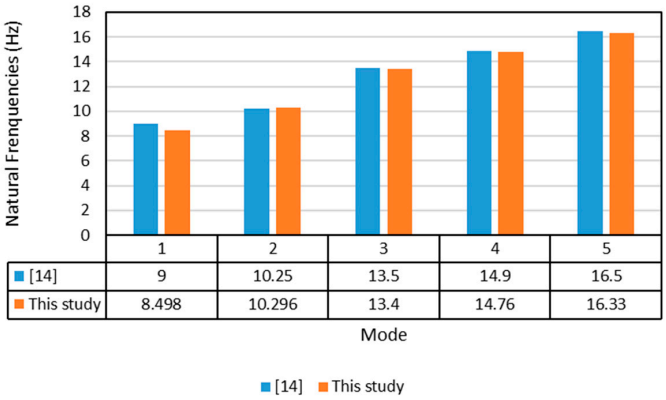

Figure 5. Comparison results of the natural frequencies of spider web structures using linear analysis.

The bar chart illustrates that the frequencies extracted from Abaqus match the results obtained from the previous study [18], and the maximum error value under linear analysis is from the comparison of mode 2, which is 5%. The comparison result verifies that the method used is reliable and can be developed further.

3. Results and Discussions

3.1. Linear Free Vibration of Spider Web

Six different spider web structures were developed to study the effects of the structural patterns and material properties including elastic modulus, inertia moment, and density.

3.1.1. Effect of Structural Patterns

There are three cases considered: the effect of a variation in radial thread number; the effect of a form of capture area; and the effect of a variation in capture thread number. Since the variation in thread number changes the mass and stiffness of the web, the natural frequencies and their fundamental mode shapes of the spider web are also changed.

Firstly, the variations of radial threads were investigated. Figure 6 presents the patterns considered in this study. The differences between these three cases are the number of radial threads. It is noted that there are 8, 12 and 16 radial threads for patterns 1, 2, 3, respectively. Figure 7 presents the natural frequencies for the spider web with a different number of radial threads. By increasing the number of radial threads, natural frequencies of different mode shape are generally increased. Mode shapes 8 and 9 have a cross over phenomenon when the patterns change from pattern 2 to pattern 3. In addition, the corresponding mode shapes of patterns 1, 2, and 3 are presented in Figure 8. It should be noted that changing the pattern by increasing the number of radial treads does not have a significant effect in lower mode as the mode shapes are almost similar for all patterns. However, it is interesting to note that the snap through behaviour, which is the jump of shape from one to another configuration, can be observed in modes 6 and 9.

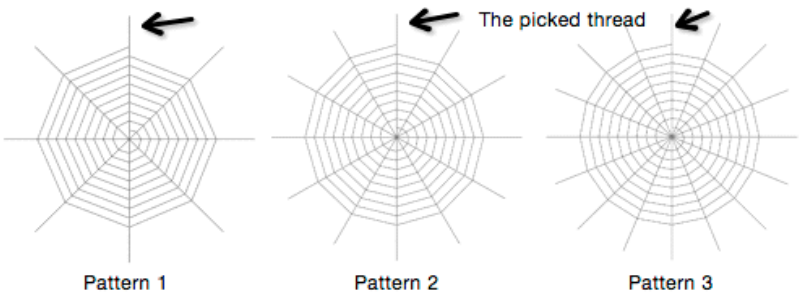

Figure 6. Patterns 1, 2 and 3 of spider web model.

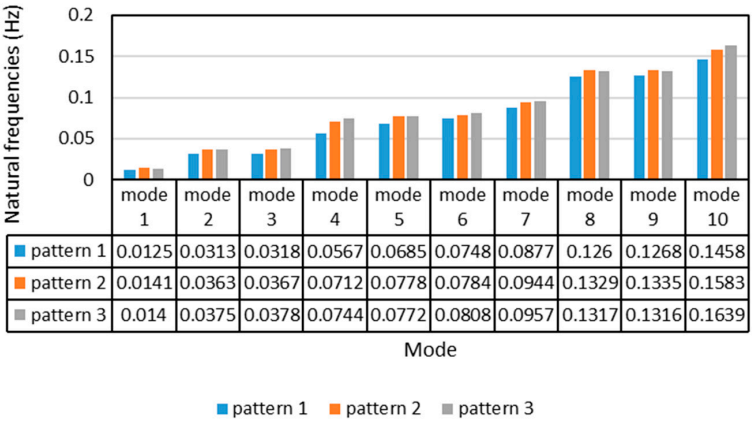

	mode 1	mode 2	mode 3	mode 4	mode 5	mode 6	mode 7	mode 8	mode 9	mode 10
pattern 1	0.0125	0.0313	0.0318	0.0567	0.0685	0.0748	0.0877	0.126	0.1268	0.1458
pattern 2	0.0141	0.0363	0.0367	0.0712	0.0778	0.0784	0.0944	0.1329	0.1335	0.1583
pattern 3	0.014	0.0375	0.0378	0.0744	0.0772	0.0808	0.0957	0.1317	0.1316	0.1639

Figure 7. Natural frequencies of spider web patterns 1, 2, and 3.

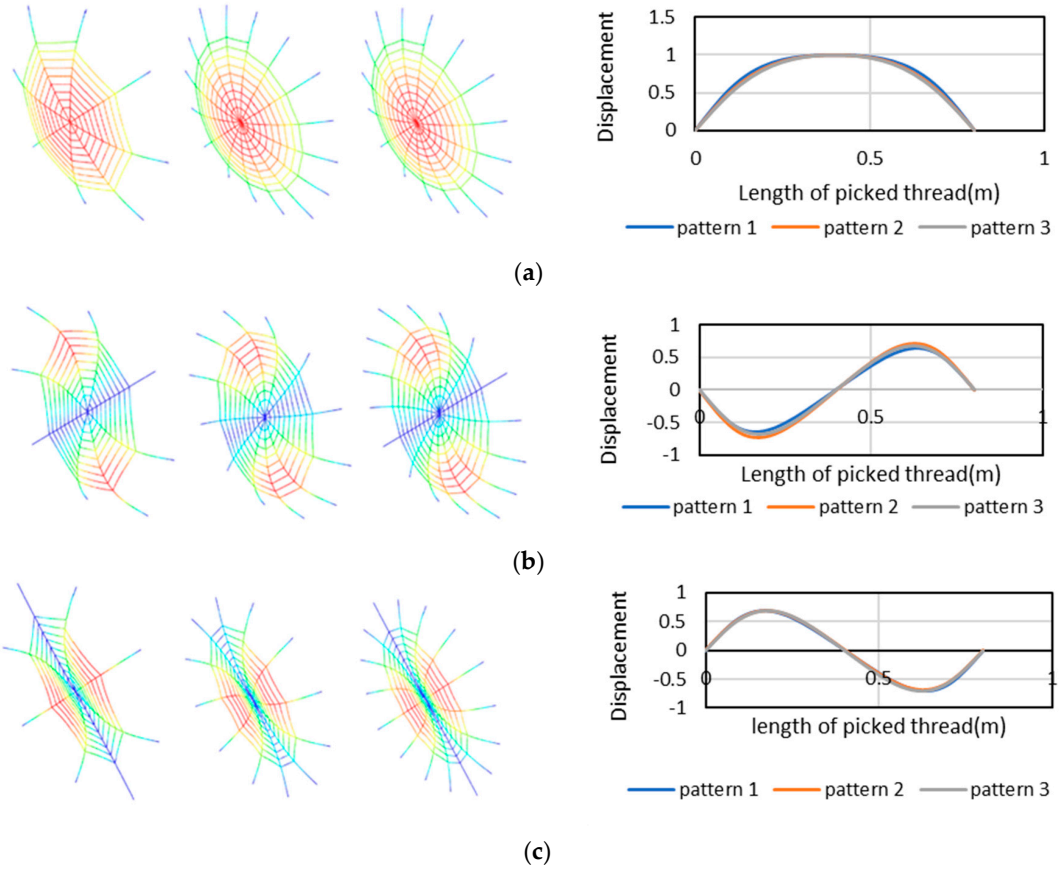

Figure 8. Mode shapes of patterns 1, 2 and 3: (**a**) mode 1(**b**) mode 2 (**c**) mode 3.

Secondly, the effects of shapes of capture threads have been considered. The patterns 1 and 4 are compared as shown in Figure 9. For pattern 1, the form of capture area is a straight spiral thread while those for pattern 4 is concentric circles. The variation of natural frequencies, influenced by the form of capture threads, is depicted in Figure 10. At the first three modes, the natural frequencies remain almost the same, but after mode 4, it becomes obvious that spider web with a straight spiral capture thread has higher natural frequencies than those with a concentric circle capture thread. It can also be explained that, as the spider web structure sustains only axial deformation, the structure with curved member could trigger the follower force and its orientation, leading to buckling behaviour so easily. This illustrates that the straight spiral thread is likely to provide more stiffness and stability to the structure rather than a circular shape of capture thread. The first three corresponding mode shapes are presented in Figure 11.

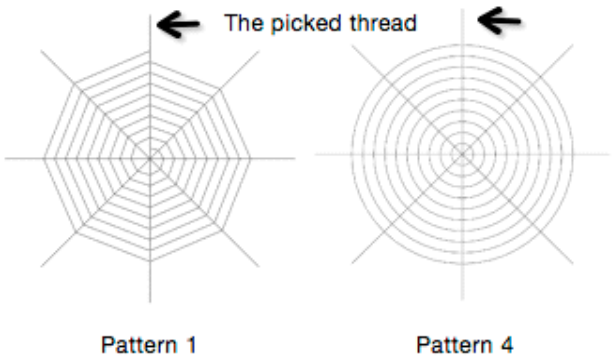

Figure 9. Patterns 1 and 4 of spider web model.

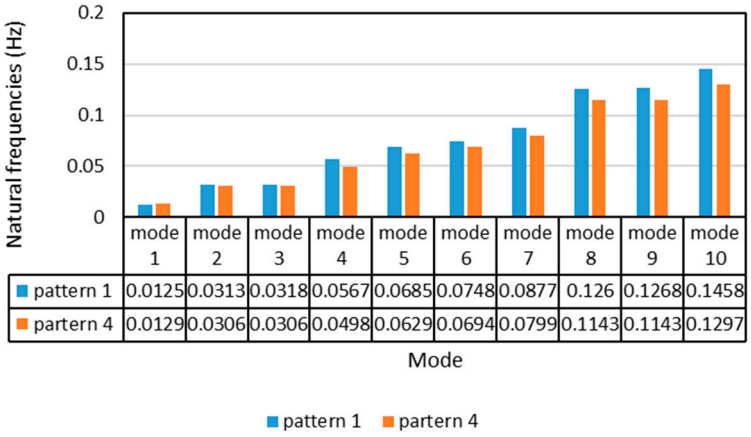

Figure 10. Natural frequencies of spider web patterns 1 and 4.

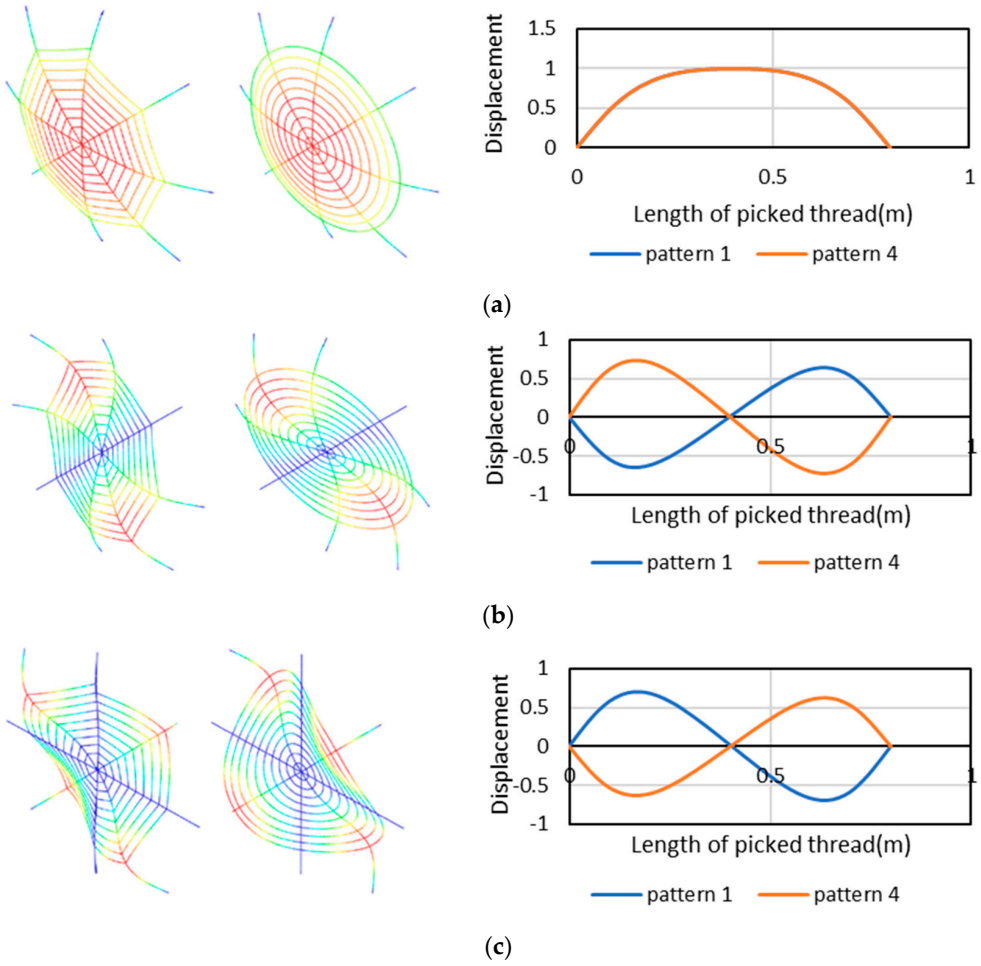

Figure 11. Mode shapes of patterns 1 and 4: (**a**) mode 1 (**b**) mode 2 (**c**) mode 3.

Moreover, the effects of the number of capture thread were studied. Figure 12 presents the patterns 4, 5, and 6 of spider web. It should be noted that there are 10, 20 and 30 capture threads for patterns 4, 5 and 6, respectively, which means that the spacing between the capture threads is 0.03, 0.015, and 0.01 m for pattern 4, 5 and 6, respectively. As the number of capture threads increases, the mesh width decreases. Figure 13 portrays the variation of natural frequencies of spider webs with the different number of capture threads. In contrast to the results of the increase in radial threads, the natural frequencies of all mode shapes are decreased while the number of capture threads increased. This sort of result shows that the increment of capture threads only significantly changes the mass of the spider

web structure, while the stiffness of the structure is not obviously affected. The corresponding mode shapes of patterns 4, 5, and 6 are compared in Figure 14. It is clear that adding more capture threads results in changing the vibration amplitude and structural stability. It is noted that snap through behaviour is observed for all modes except for modes 1, 7 and 10. As aforementioned, the straight spiral thread is the optimum geometry of spider web with stronger structural stability than concentric circles capture area. In other words, in comparison to spiral capture area, the spider web with the concentric circles capture area is not that stable and the increase in capture threads does not obviously strengthen the stability of the spider web structure.

By comparing the frequencies of different the spider web patterns, it can be concluded that the capture threads play a non-structural role as adding more capture threads results in decreasing the natural frequencies. Where radial threads are treated as structural members, they can increase the stiffness of the structure rather than mass, showing the improvement ostructural stability.

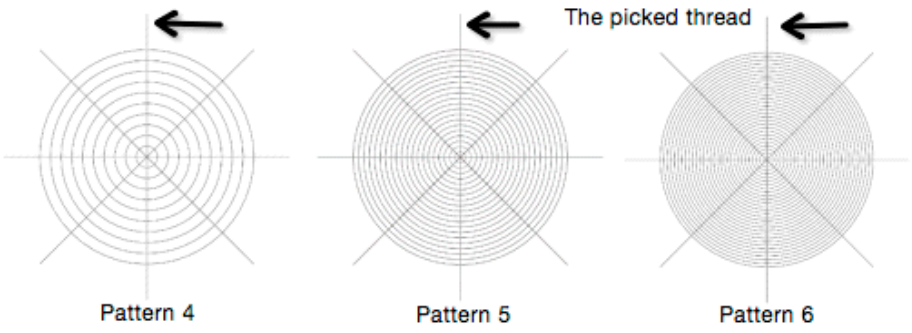

Figure 12. Patterns 4, 5 and 6 of spider web model.

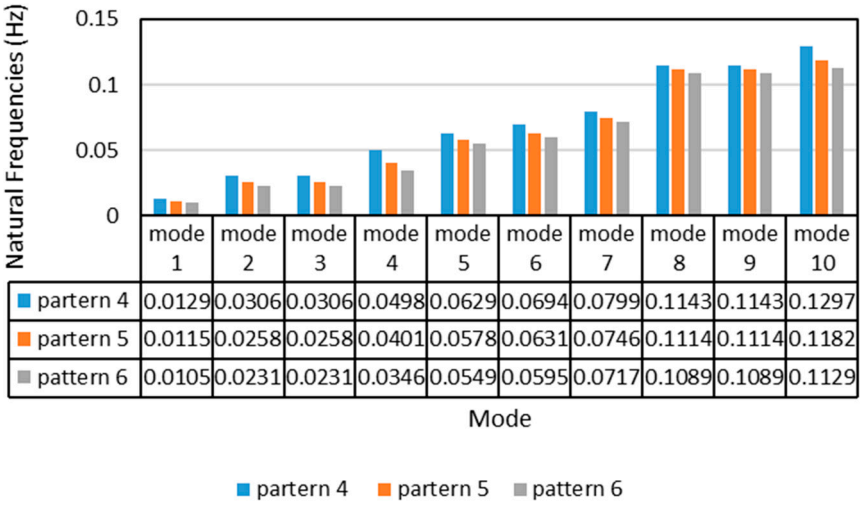

	mode 1	mode 2	mode 3	mode 4	mode 5	mode 6	mode 7	mode 8	mode 9	mode 10
partern 4	0.0129	0.0306	0.0306	0.0498	0.0629	0.0694	0.0799	0.1143	0.1143	0.1297
partern 5	0.0115	0.0258	0.0258	0.0401	0.0578	0.0631	0.0746	0.1114	0.1114	0.1182
pattern 6	0.0105	0.0231	0.0231	0.0346	0.0549	0.0595	0.0717	0.1089	0.1089	0.1129

Figure 13. Natural frequencies of spider web patterns 4, 5, and 6.

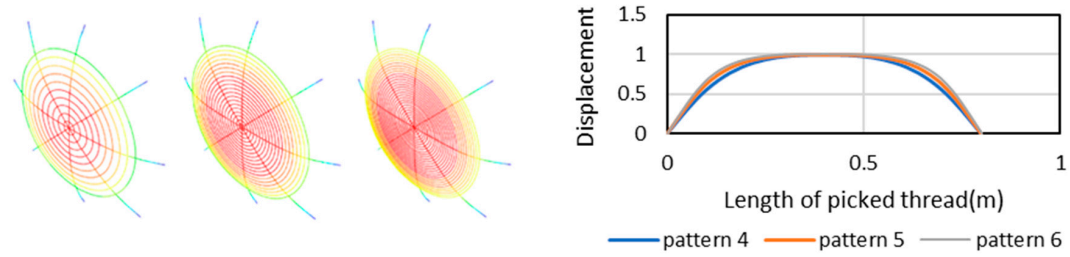

(**a**)

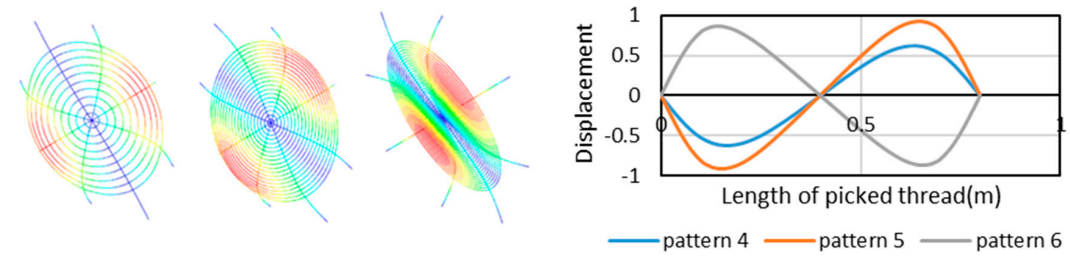

(**b**)

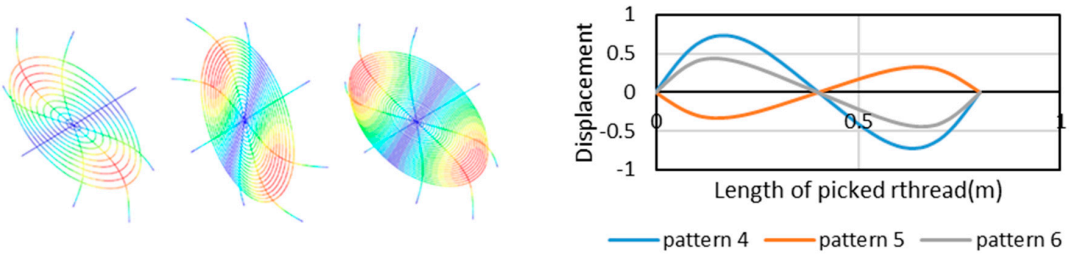

(**c**)

Figure 14. Mode shapes of patterns 4, 5 and 6: (**a**) mode 1 (**b**) mode 2 (**c**) mode 3.

3.1.2. Effect of Elastic Modulus

In this section, pattern 1 has been chosen for the parametric studies. Figure 15 displays the results for natural frequencies of the spider web with different elastic moduli. In this parametric study, the original elastic modulus of radial and spiral threads is 34 GPa and changed by increasing or decreasing by 10% of 34 GPa at each step. It is clear in Figure 15 that by increasing the elastic modulus, natural frequencies of spider web structure are increased, which contributes to the addition of stiffness. As the elastic modulus is doubled, the natural frequencies are accordingly increased by 1.4 times.

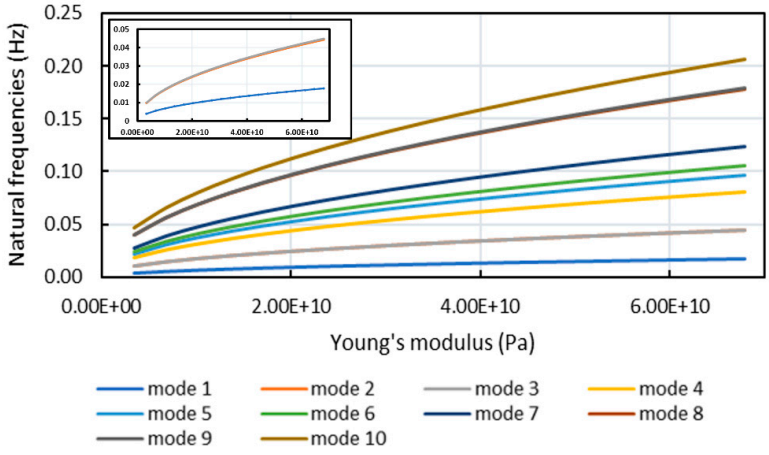

Figure 15. Natural frequencies of spider web with elastic modulus.

3.1.3. Effect of Inertia Moment

As previously mentioned, a single spider silk thread is considered as a cable segment which has negligible torsional, bending and shear rigidities. Therefore, the inertia moment of material should be very small, which can be considered as zero. In ABAQUS, the inertia moment cannot be set as zero; however, the area of cross-section of spider silk, which is a direct proportion to the moment of inertia, is already very small (4 microns) in this model. However, the inertia moment still can be reduced within a limited range to investigate the tendency of natural frequencies with low inertia moment. It is noted that the original value of the inertia moment is 1.256×10^{-23} Pa. Figure 16 shows the variation of natural frequencies which are influenced by the inertia moment. The natural frequencies decreased as the inertia moment reduced. It is noticeable that mode shapes 6 and 7 have a cross over at the point where the value of inertia moment is 3.55×10^{-24}. This is due to the structural instability caused by the change in material properties.

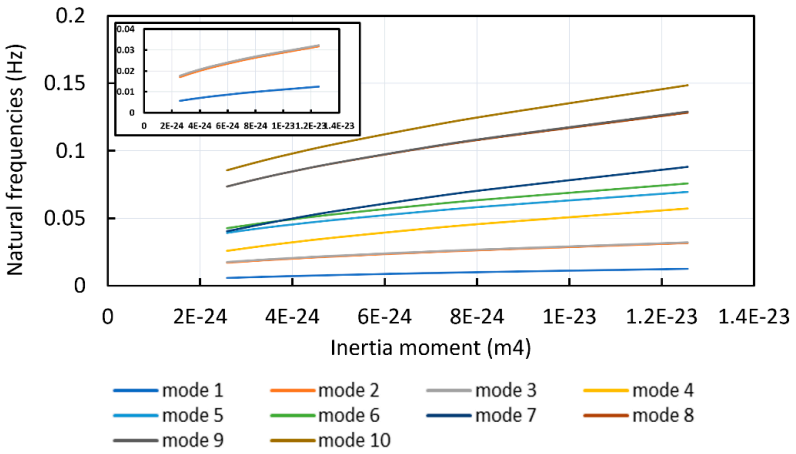

Figure 16. Natural frequencies of spider web with inertia moment.

3.1.4. Effect of Density

The mass of the structure is changed along with the change in the density, which would affect the natural frequencies. It should be noted that the density of a spider web is generally varied from about 900 to 1600 kg/m^3 [4]. However, this study considers from the realistic value until the significant changes in natural frequencies are observed. Figure 17 illustrates the tendency of the change in natural frequencies affected by structural density. By increasing the density, the natural frequencies of spider web are generally reduced. The density has a significant effect on natural frequencies, especially when the density is low. However, with the density becoming larger, the trend of this change in natural frequencies becomes smoother.

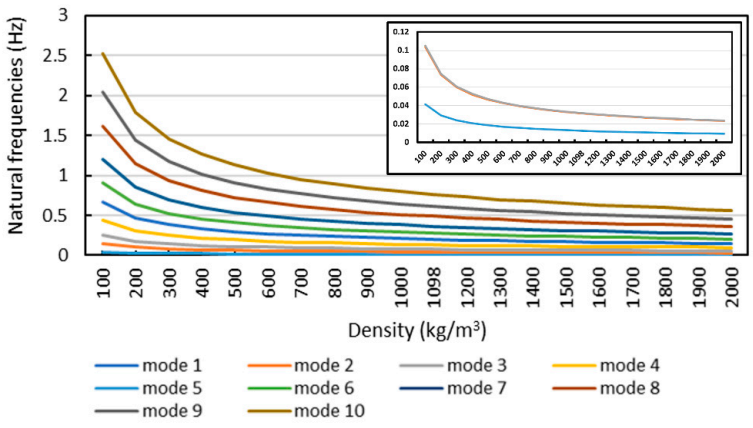

Figure 17. Natural frequencies of spider web with density.

It should also be noted that the Young's modulus, inertia moment, and density do not significantly affect the lower modes. However, they can slightly affect the higher modes, as the cross over phenomenon can be observed, especially when the moment of inertia changed.

3.2. Nonlinear Free Vibration of Spider Web

Large amplitude free vibration of spider webs with geometry nonlinearity is investigated, considering pattern 1. During the process via iterative solution, the stiffness is updated due to the large deformation. This part investigates the significance of geometrically nonlinear analysis with the pretension loads. It should be noted that the pretension loads are applied to create a nonlinear displacement-strain situation as the initial condition. This section includes the study of natural frequencies and corresponding mode shapes and parametric study of the effect of Young's modulus and density. Figure 18 shows the natural frequencies of spider webs under different pretension loads. It can be seen that, as the pretension load increases, the natural frequencies increase gently as well. This is because, along with the growth of the pretension load, the stiffness of the whole structure is improved, as a result of geometric nonlinearity. It is found that mode shapes 8 and 9 are crossed over at the pretension load between 1.5625×10^{-7} and 7.8125×10^{-7} N. However, the fundamental frequencies are quite close, so that the cross over phenomenon is hardly seen in Figure 18. This occurrence is attributed to the fact that the hardening phenomenon can influence the performance of spider web structure. Figure 19 depicts the nonlinear frequency ratio $(\omega_N/\omega_L)^2$ of the spider web and it shows that the nonlinear vibrational behaviour of the spider web is also categorised into the hardening state, especially at mode 1. The nonlinear frequencies are compared with the corresponding linear frequencies that have been analysed previously. In this study, the pretension force is varied from 10^{-11} to 10^{-5} N as the initial condition. The results are presented in terms of pretension load ratio (pretension force/10^{-11}) and frequency ratio (Nonlinear frequency/linear frequency).

As the pretension load applied to the structure increases, the whole structure becomes hardening and the amplitudes of vibrations of all modes are decreased gradually. When the pretension load applied to 7.8125×10^{-7} N, the hardening level is highest and the fall of the amplitude of free vibration is mostly obvious. It has to be pointed out that the modes 2, 3, 7 and 10 have a snap through. The model vibrates back and forth, and as the stiffness of the structure is changed due to the geometric nonlinearity, the natural frequencies are changed. Hence, structural stability is influenced by the effect of consideration of geometric nonlinearity. Once the structure becomes unstable, there is a snap through behaviour.

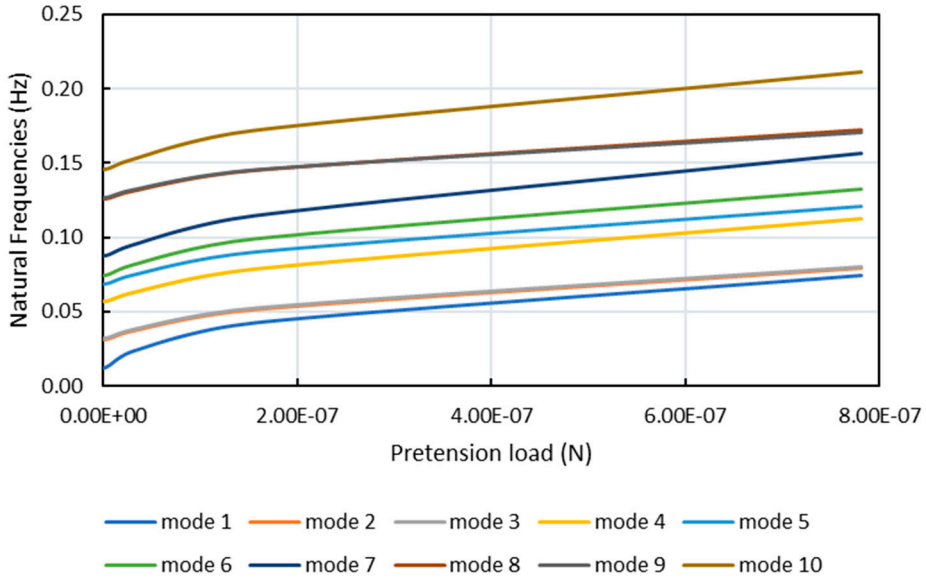

Figure 18. Natural frequencies of spider web under different pretension loads.

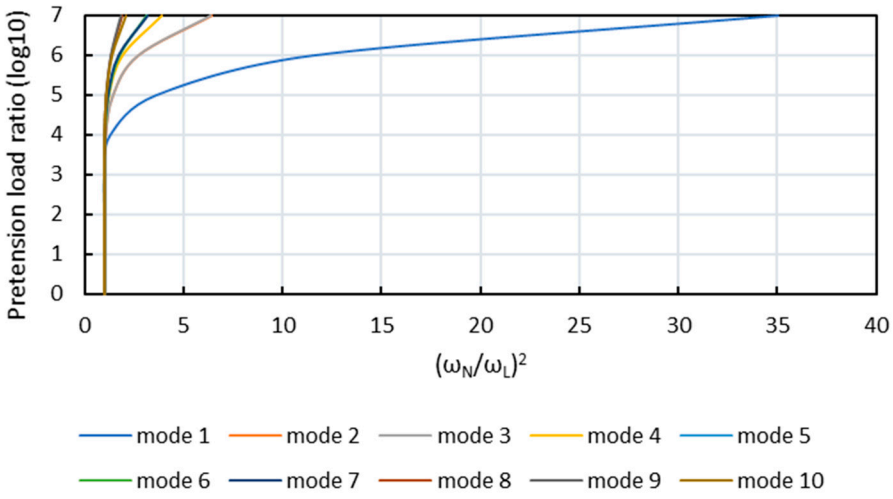

Figure 19. Frequency ratio $(\omega_N/\omega_L)^2$ of spider web under different pretension loads.

Effects of Elastic Modulus and Density

In this section, the effects of Young's modulus and density of spider web are considered with the variation of pretension load. The variation of the nonlinear frequency ratio $(\omega_N/\omega_L)^2$, influenced by the elastic modulus, is depicted in Figure 20. Obviously, the elastic modulus significantly affects the nonlinear frequency. It can be seen, as the elastic modulus reduced, that the degree of hardening increases in all mode shape. It is noted that the spider web is more sensitive to pretension load and the hardening phenomenon is more obvious when the elastic modulus is low. In other words, with the lower Young's modulus, the structure will lose its characteristic of elastic deformation easier, even when subjected to a small load. Mode shape 1 has the most obvious hardening phenomenon in comparison to other modes.

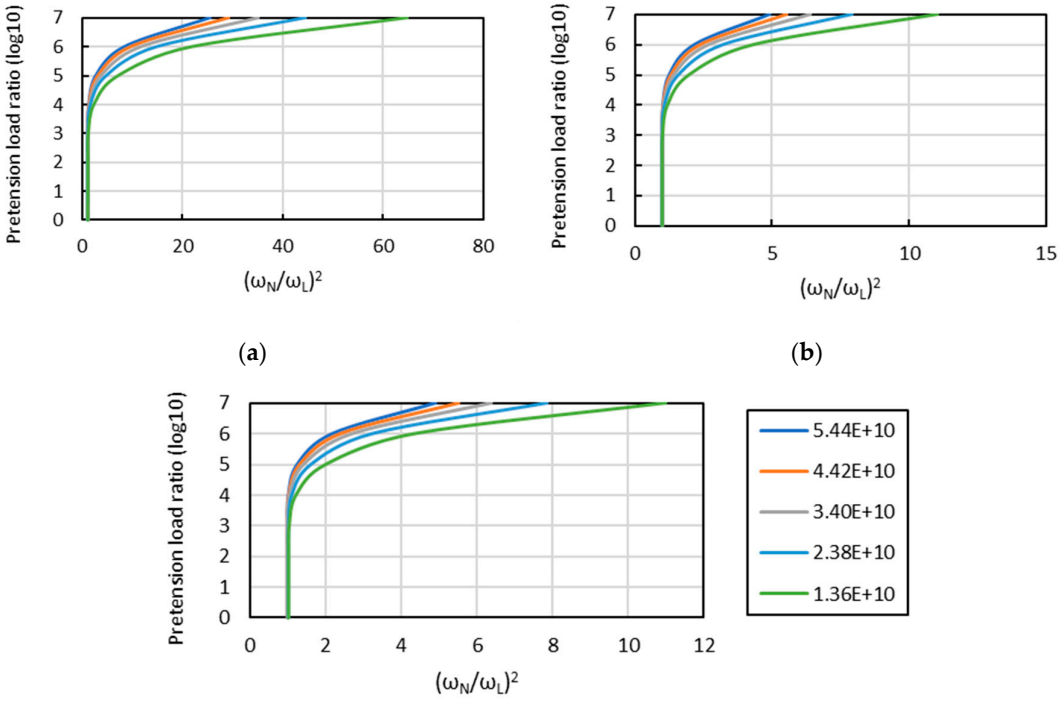

Figure 20. Effect of elastic moduli on the nonlinear frequency ratios $(\omega_N/\omega_L)^2$ and pretension load ratio for: (**a**) mode 1 (**b**) mode 2 (**c**) mode 3.

From Figure 21, it needs to be mentioned that there is a cross over between mode shapes 8 and 9 when the elastic modulus decreases to 2.38×10^{10} Pa and a cross over between modes 7, 8 and 9 when the elastic modulus decreases to 1.36×10^{10} Pa. This is because the structure becomes unstable as the hardening phenomenon becomes more obvious during the pretension loads between 1.5621×10^{-7} and 7.8125×10^{-7} N. The high degree of hardening affects the stability of the structure, especially at the lower elastic modulus, where this affection is more significant.

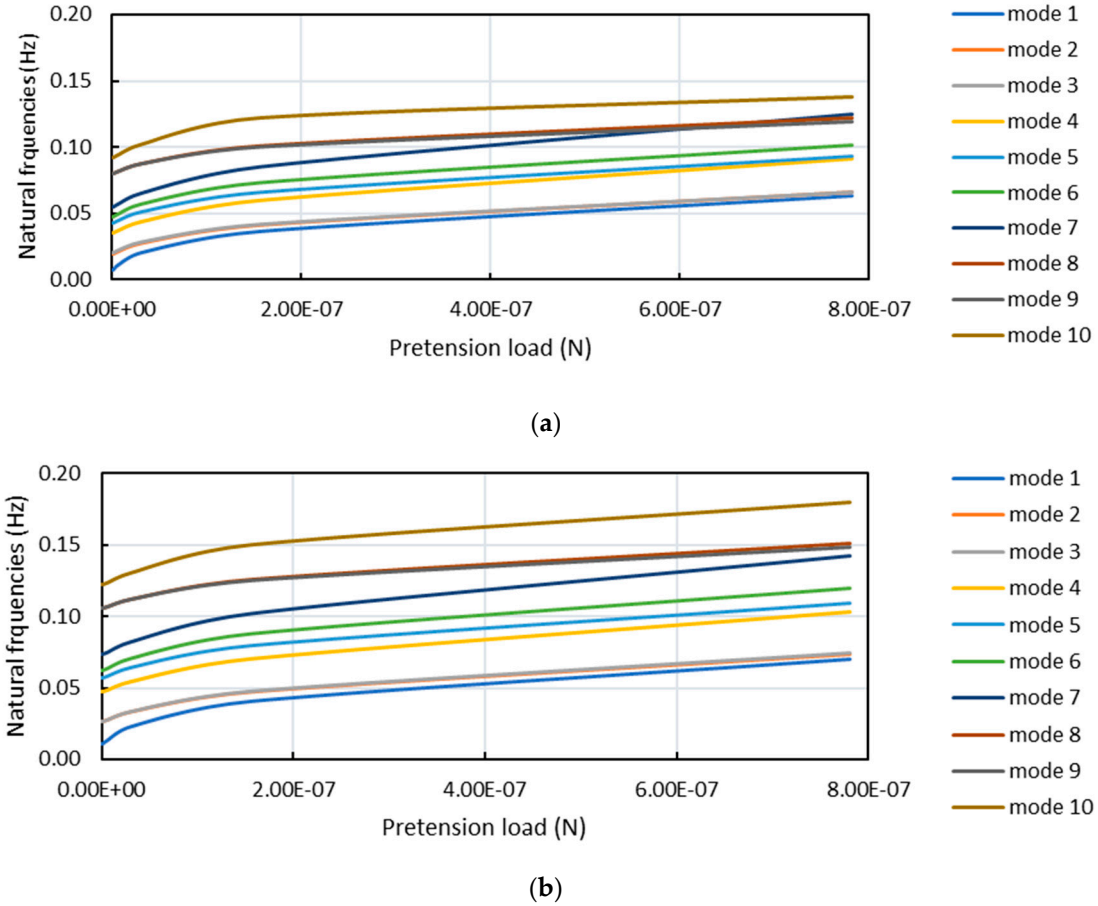

Figure 21. Natural frequencies with different pretension loads and elastic moduli: (**a**) E = 1.36×10^{10} Pa (**b**) E = 2.38×10^{10} Pa.

Figure 22 demonstrates the nonlinear frequency ratio $(\omega_N/\omega_L)^2$ considering the variation of the density of the spider web. It is clearly seen that the density also plays a role in structural stability as the structure easily exhibits the hardening state when the density is increased. These nonlinear phenomena are similar to the dynamic behaviours of highly slender structures [19–21]. However, it is noted that the cross over phenomenon is not observed.

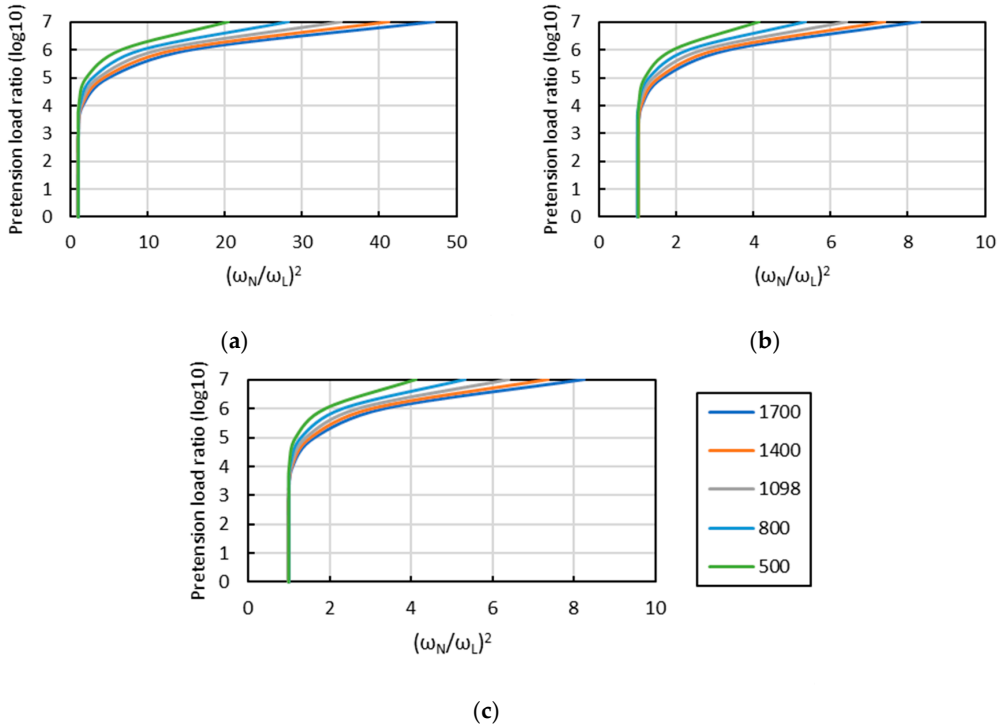

Figure 22. Effect of density on the nonlinear frequency ratio $(\omega_N/\omega_L)^2$ and pretension load ratio for (**a**) mode 1 (**b**) mode 2 (**c**) mode 3.

4. Conclusions

This paper presents the investigation of natural frequencies and the corresponding mode of spider web under different conditions. The analysis includes the consideration of structural shape and geometric nonlinearity. The different patterns indicate that the increase in radial threads indeed improves the stiffness of the whole structure, while the increase in capture threads increases the mass of the structure. This implies that the radial threads play a significant role in the structural performance and are structural members, whereas the capture threads represent non-structural members. The effects of material properties including elastic modulus, inertia moment and density are also investigated. These properties significantly affect the natural frequencies and the crossover phenomenon can be observed in higher modes of vibration. Due to the change in structural pattern and material properties, the characteristics of the structure itself have been influenced, such as the structural stability and the stiffness. This explains why the crossover phenomenon of frequencies between two different mode shapes and the snap through behaviour exist. It is noted that nonlinearity has a strong influence on spider web structure. By increasing the pretension load, the nonlinear vibration behaviour is categorised into the hardening state. The outcome of this study will help a structural engineer to adapt the concept of spider web's structure and its properties in the design of any larger structures.

Author Contributions: Conceptualisation, S.K.; methodology, S.K.; software, C.N. and T.Y.; validation, C.N., and T.Y.; formal analysis, T.Y.; investigation, S.K., C.N. and T.Y.; resources, S.K.; writing—original draft preparation, C.N.; writing—review and editing, S.K. and C.N.; visualisation, T.Y.; supervision, S.K.; project administration, S.K.; funding acquisition, S.K. All authors have read and agreed to the published version of the manuscript.

Funding: This research was funded by the European Commission for the H2020-RISE Project No. 691135 "RISEN: Rail Infrastructure Systems Engineering Network". The APC is sponsored by the University of Birmingham Library's Open Access Fund.

Acknowledgments: The authors are sincerely grateful to European Commission for the financial sponsorship of the H2020-MSCA-RISE Project No. 691135 "RISEN: Rail Infrastructure Systems Engineering Network," which enables a global research network that tackles the grand challenge of railway infrastructure resilience and advanced sensing in extreme environments (www.risen2rail.eu) [22].

Conflicts of Interest: The authors declare no conflict of interest.

References

1. Römer, L.; Scheibel, T. The elaborate structure of spider silk: Structure and function of a natural high performance fiber. *Prion* **2008**, *2*, 154–161. [CrossRef] [PubMed]
2. Saravanan, D. Spider silk-structure, properties and spinning. *J. Text. Appar. Technol. Manag.* **2006**, *5*, 1–20.
3. Vierra, C.; Hsia, Y.; Gnesa, E.; Tang, S.; Jeffery, F. Spider silk composites and applications. In *Metal, Ceramic and Polymeric Composites for Various Uses*; IntechOpen: London, UK, 2011.
4. Ko, F.K.; Jovicic, J. Modeling of mechanical properties and structural design of spider web. *Biomacromolecules* **2004**, *5*, 780–785. [CrossRef] [PubMed]
5. Du, N.; Yang, Z.; Liu, X.Y.; Li, Y.; Xu, H.Y. Structural origin of the strain-hardening of spider silk. *Adv. Funct. Mater.* **2011**, *21*, 772–778. [CrossRef]
6. Kelly, S.P.; Sensenig, A.; Lorentz, K.A.; Blackledge, T.A. Damping capacity is evolutionarily conserved in the radial silk of orb-weaving spiders. *Zoology* **2011**, *114*, 233–238. [CrossRef] [PubMed]
7. Sensenig, A.; Agnarsson, I.; Blackledge, T.A. Behavioural and biomaterial coevolution in spider orb webs. *J. Evol. Biol.* **2010**, *23*, 1839–1856. [CrossRef] [PubMed]
8. Sensenig, A.T.; Kelly, S.P.; Lorentz, K.A.; Lesher, B.; Blackledge, T.A. Mechanical performance of spider orb webs is tuned for high-speed prey. *J. Exp. Biol.* **2013**, *216*, 3388. [CrossRef] [PubMed]
9. Cranford, S.W.; Tarakanova, A.; Pugno, N.M.; Buehler, M.J. Nonlinear material behaviour of spider silk yields robust webs. *Nature* **2012**, *482*, 72–76. [CrossRef] [PubMed]
10. Gosline, J.M.; DeMont, M.E.; Denny, M.W. The structure and properties of spider silk. *Endeavour* **1986**, *10*, 37–43. [CrossRef]
11. Moore, A.M.F.; Tran, K. Material properties of cobweb silk from the black widow spider latrodectus hesperus. *Int. J. Biol. Macromol.* **1999**, *24*, 277–282. [CrossRef]
12. Ko, F.K.; Kawabata, S.; Inoue, M.; Niwa, M.; Fossey, S.; Song, J.W. Engineering properties of spider silk. *MRS Online Proc. Libr. Arch.* **2001**, *702*, 1–7. Available online: https://web.mit.edu/3.064/www/slides/Ko_spider_silk.pdf (accessed on 1 August 2020). [CrossRef]
13. Qin, Z.; Compton, B.G.; Lewis, J.A.; Buehler, M.J. Structural optimization of 3d-printed synthetic spider webs for high strength. *Nat. Commun.* **2015**, *6*, 7038. [CrossRef]
14. Tietsch, V.; Alencastre, J.; Witte, H.; Torres, F.G. Exploring the shock response of spider webs. *J. Mech. Behav. Biomed. Mater.* **2016**, *56*, 1–5. [CrossRef] [PubMed]
15. Srinil, N.; Rega, G.; Chucheepsakul, S. Three-dimensional non-linear coupling and dynamic tension in the large-amplitude free vibrations of arbitrarily sagged cables. *J. Sound Vib.* **2004**, *269*, 823–852. [CrossRef]
16. Kwan, A.S.K. Mechanics and Structure of Spider Webs. In Proceedings of the Seventh International Conference on Computational Structures Technology, Lisbon, Portugal, 7–9 September 2004; Topping, B.H.V., Soares, C.A.M., Eds.; Civil-Comp Press: Stirling, UK, 2005.
17. Moideen, K.K.R.; Dewangan, U.K. Comparative study of linear and geometric nonlinear load-deflection behaviour of flexural steel members. *Indian J. Sci. Technol.* **2016**, *9*, 1–6.
18. Zheng, L.; Behrooz, M.; Li, R.; Wang, X.; Gordaninejad, F. Performance of a Bio-Inspired Spider Web. Proceedings of SPIE—The International Society for Optical Engineering. 2014. Available online: https://www.spiedigitallibrary.org/conference-proceedings-of-spie/9057/90570I/Performance-of-a-bio-inspired-spider-web/10.1117/12.2046379.short?SSO=1 (accessed on 31 July 2020).
19. Kaewunruen, S.; Chiravatchradej, J.; Chucheepsakul, S. Nonlinear free vibrations of marine risers/pipes transporting fluid. *Ocean Eng.* **2005**, *32*, 417–440. [CrossRef]
20. Chucheepsakul, S.; Kaewunruen, S.; Suwanarat, A. Large deflection analysis of orthotropic, elliptic membranes. *Struct. Eng. Mech.* **2009**, *31*, 6, 625–638. [CrossRef]
21. Sengsri, S.; Kaewunruen, S. Additive manufacturing meta-functional composites for engineered bridge bearings: A review. *Construct. Build. Mat.* **2020**, in press. [CrossRef]
22. Kaewunruen, S.; Sussman, J.M.; Matsumoto, A. Grand challenges in transportation and transit systems. *Front. Built Environ.* **2016**, *2*, 4. [CrossRef]